Japanese Journal of Applied Physics **54**, 08KA04 (2015) **REGULAR PAPER**
http://dx.doi.org/10.7567/JJAP.54.08KA04

Control of intermediate-band configuration in GaAs:N δ-doped superlattice

Kazuki Osada[1]*, Tomoya Suzuki[1], Shuhei Yagi[1]*, Shunya Naitoh[2], Yasushi Shoji[2], Yasuto Hijikata[1], Yoshitaka Okada[2], and Hiroyuki Yaguchi[1]

[1]*Graduate School of Science and Engineering, Saitama University, Saitama 338-8570, Japan*
[2]*Research Center for Advanced Science and Technology (RCAST), The University of Tokyo, Meguro, Tokyo 153-8904, Japan*
E-mail: osadak@opt.ees.saitama-u.ac.jp; yagi@opt.ees.saitama-u.ac.jp

Received December 19, 2014; revised February 24, 2015; accepted February 25, 2015; published online July 3, 2015

GaAs:N δ-doped superlattices (SLs) consisting of alternating layers of undoped and N δ-doped GaAs were fabricated by molecular beam epitaxy (MBE) as possible candidates for the light-absorbing material of intermediate-band solar cells (IBSCs). Since the energy gaps in IBSCs need to be adjusted to optimum values to achieve sufficiently high conversion efficiency, it is important to control precisely the band configuration of intermediate-band (IB) materials. In this study, we demonstrated the control of the IB energy configuration in GaAs:N δ-doped SLs by changing their structural parameters. Optical transitions due to the SL minibands related to the N-induced conduction subbands E_+ and E_- were clearly observed and the transition energies depended systematically on the N area density and period length of the SLs. Conversion efficiency calculations based on the detailed balance model indicated that IBSCs with an efficiency of nearly 60% are achievable by using the fabricated GaAs:N δ-doped SLs.

1. Introduction

The development of intermediate-band solar cells (IBSCs) is an attempt to improve photovoltaic power generation efficiency.[1–12] GaAsN is a possible candidate light-absorbing material of IBSCs because the N-induced conduction subbands E_+ and E_- formed in GaAsN are considered to compose an intermediate-band (IB) structure with the valence band (VB).[13–18] However, in general, the optical transition originating from the E_+ band is not as clearly observed as one from the E_- band.[19–23] In our previous work, we found that superlattice (SL) structures consisting of alternating layers of undoped and N δ-doped GaAs show stronger optical transitions originating from SL minibands related to the E_+ band than those from the E_+ band in conventional GaAsN alloys.[24–26] In such GaAs:N δ-doped SLs, each of the E_+ and E_- bands formed around the N δ-doped layers composes SL potentials with the conduction band (CB) of spacer GaAs, resulting in the formation of minibands related to E_+ and E_- bands above and below the GaAs CB edge, respectively.[24] These E_+ and E_- minibands are originally from energetically separated conduction subbands, and thus are considered to compose an ideal IB structure. On the basis of their superior optical properties, we propose the SLs as more promising candidate IB absorbers.[25]

According to the detailed balance theory of IBSCs, the energy gaps in the IB absorber need to be optimized to achieve a sufficiently high conversion efficiency.[1] Therefore, it is important to control precisely the band energy configuration in IB materials. The IB energy configuration in GaAs:N δ-doped SLs is determined on the basis of the SL potentials originating from the N-induced conduction subbands and therefore is expected to show systematic dependence on structural parameters such as the N area density in δ-doped layers and period lengths of the SLs.[25] In this report, we experimentally demonstrate the control of energy configuration of the IB structure in GaAs:N δ-doped SLs by adjusting structural parameters.

2. Experimental methods

GaAs:N δ-doped SLs with nominal SL periods of 9, 6, and 4 nm were fabricated by molecular beam epitaxy (MBE) on GaAs(001) substrates. Metal Ga and As were used as the Ga and As sources, respectively. A valved cracker cell was used to supply As and was operated in the As_2 mode. Active N was supplied by an rf plasma source. A GaAs buffer layer was grown on a substrate at 580 °C followed by the growth of a 20-period SL of GaAs:N δ-doped layers at 500 °C. A N δ-doped layer was formed by supplying active N during the growth interruption and the following GaAs growth. The area density of N in a δ-doped layer was controlled by changing the duration of the N supply. A 20-nm-thick GaAs cap layer was grown on top of the SL. The sample structures were evaluated by cross-sectional transmission electron microscopy (TEM) and X-ray diffraction (XRD). The SL period and average N composition in the SLs were measured by θ–2θ XRD scans, and the N area density in a δ-doped layer was estimated from these data. Photoreflectance (PR) measurements were carried out at 120 K to investigate the energy configuration of the SLs. In the PR measurements, a diode-pumped solid-state (DPSS) laser at 532 nm was used to provide the pump beam. A probe light was obtained from a halogen lamp, the emission from which was dispersed through a monochromator. PR signals were detected by a Si photodiode. To investigate the origin of the enhanced optical transitions related to the E_+ band in the SLs, some samples were subjected to rapid thermal annealing in N_2 atmosphere at several temperatures, and structural and optical characterizations were carried out.

3. Results and discussion

XRD measurements revealed that the N area density in a δ-doped layer of the obtained SLs was well controlled in the range from $\sim 4 \times 10^{13}$ to $2 \times 10^{14}\,cm^{-2}$ by changing the N exposure time during the formation of N δ-doped layers. The SL period was estimated from the 1st-order satellite peak positions in the XRD patterns around the GaAs(004) peak, and the deviation from the nominal values was within 0.3 nm for all the samples. A cross-sectional TEM image of a GaAs:N δ-doped SL with a period of 6.2 nm and N area density of $1.9 \times 10^{14}\,cm^{-2}$ is presented in Fig. 1. The average N composition in the SL region of this sample was 1.36%.

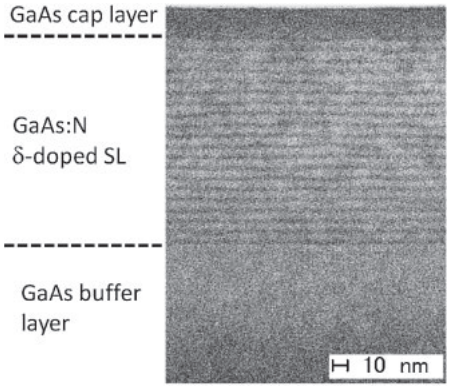

Fig. 1. Cross-sectional TEM image of a GaAs:N δ-doped SL with a period of 6.2 nm and a N area density of $1.9 \times 10^{14}\,cm^{-2}$.

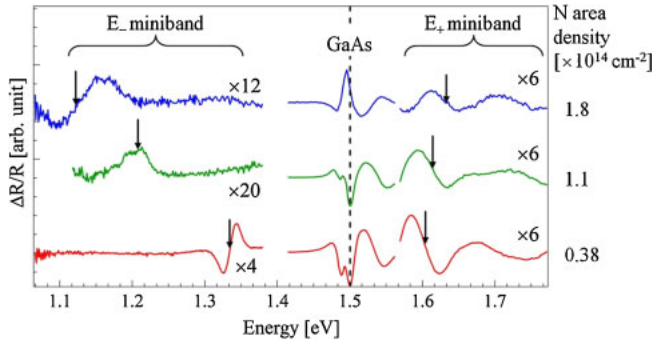

Fig. 2. (Color online) PR spectra of GaAs:N δ-doped SLs with a nominal period of 4 nm. The PR measurements were carried out at 120 K.

No misfit dislocations were observed throughout the SL structure, and fine formation of a periodic structure in the growth direction was confirmed, as shown in the figure.

Figure 2 shows PR spectra of GaAs:N δ-doped SLs with the nominal SL period of 4 nm. The N area density in a δ-doped layer of these samples was in the range from 0.38×10^{14} to $1.8 \times 10^{14}\,cm^{-2}$. Aside from the GaAs bandgap transitions near 1.5 eV originating from the cap layer, buffer layer, and/or substrate, several transitions were observed in the PR spectra for all the SLs. The PR signals above and below the GaAs bandgap energy were due to optical transitions from the VB to SL minibands related to the E_+ and E_- bands, respectively. The arrows in Fig. 2 indicate the energy positions of the E_+ and E_- miniband bottoms estimated from fitting with Aspnes' third derivative functional form.[27] As the N area density increased, the transition energy related to the E_+ miniband increased, and that to the E_- miniband decreased. As stated in the introduction, the SL potentials are composed of N-induced conduction subbands in the vicinity of the N δ-doped layers and the CB of spacer GaAs. Since the E_+ and E_- bands locate above and below the GaAs CB, respectively, the E_+ band behaves as the barrier whereas the E_- band behaves as the well in the SL potential. In either case, the dependence of the SL miniband energy on the N content should have a tendency similar to that of the conduction subband that composes the SL. The energies of the E_+ and E_- bands in GaAsN increases and decreases with increasing N content, respectively. Therefore, the behaviors of the miniband energies observed in the PR spectra are considered reasonable.

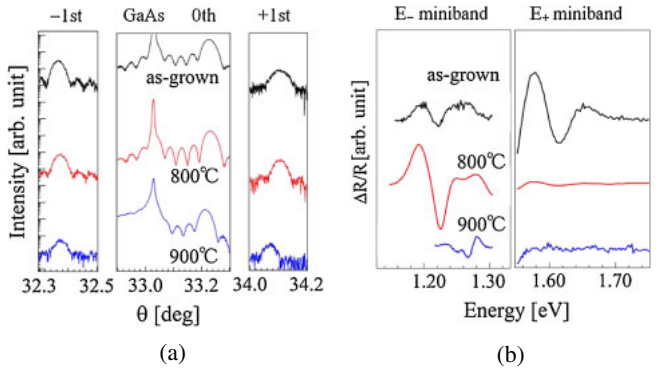

Fig. 3. (Color online) (a) XRD patterns and (b) PR spectra of a GaAs:N δ-doped SL with a SL period of 6 nm and a N area density of $1.1 \times 10^{14}\,cm^{-2}$ measured before and after annealing. PR measurements were carried out at 120 K.

The signal intensity of the E_+ band transitions of conventional GaAsN alloys in modulation spectroscopies is typically one order of magnitude lower than that of the E_- band transition.[19–23] Thus, the oscillator strength deduced from the PR signal intensity for the E_+ miniband transitions in the SLs is relatively larger than that for the E_+ band transitions in conventional GaAsN alloys. To investigate the origin of the enhanced optical transitions related to the E_+ band in the SLs, annealing characteristics were evaluated. Figure 3(a) shows XRD patterns of as-grown and annealed SLs with a SL period of 6.2 nm and a N area density of $1.1 \times 10^{14}\,cm^{-2}$. The annealing was carried out at 800 and 900 °C for 5 min. As the annealing temperature increased, the intensity of the SL satellite peak decreased, implying that the abruptness of N distribution in the δ-doped layers was decreased owing to the thermal diffusion. Note that the position of the 0th-order satellite peak did not move after the annealing, and thus the total N content in the SL was maintained. Figure 3(b) shows corresponding PR spectra of these samples. Moderate thermal treatments often improve the crystal quality and optoelectronic properties of dilute nitride alloys,[28–32] and this can account for the increase in the PR signal intensities for E_--related transition at about 1.2 eV after the annealing at 800 °C. The slight increase in the transition energy of the E_--related transition after 900 °C may originate from changes in the SL potential owing to the broadening of the N distribution profile. The E_+-related transition signals in an energy range from 1.55 to 1.8 eV for the as-grown SL are more intense than the E_--related transition signals. The E_+-related signals became significantly weaker or disappeared after annealing. Therefore, it can be assumed that the abrupt distribution of N in δ-doped layers contributes to the enhancement of the E_+-related transitions and that the oscillator strengths of these transitions are much more sensitive to the N distribution than those of the E_--related transitions.

Finally, the energy positions of the miniband bottoms of the SLs estimated from PR transition signals are plotted in Fig. 4 as a function of the N area density in a δ-doped layer. The results for the SLs with nominal periods of 4, 6, and 9 nm are indicated in the figure. Both transition energies related to the E_+ and E_- minibands depended on the N area density, as shown earlier. In addition, although the difference is not as large, the shorter SL period causes the lower

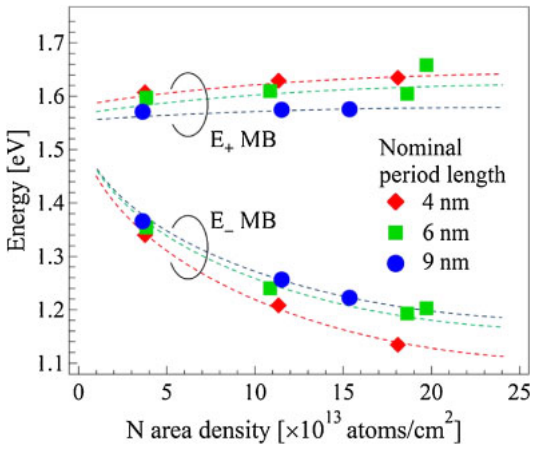

Fig. 4. (Color online) Dependence of the miniband (MB) bottom energies of GaAs:N δ-doped SLs on the SL period and N area density. The dotted lines are a guide to the eye.

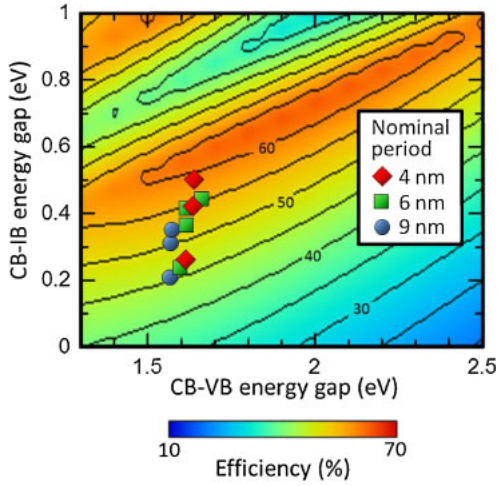

Fig. 5. (Color online) Calculated conversion efficiency of IBSCs as a function of the CB–VB gap energy and the CB–IB gap energy. The closed symbols indicate the energy gap relations of the fabricated SLs in which the bottom energies of the E_+ and E_- minibands estimated by PR are assumed to correspond to those of the CB and IB, respectively.

transition energies of the E_--related miniband and the higher transition energies of the E_+-related miniband. Therefore, it is demonstrated that the energy configurations in GaAs:N δ-doped SLs are successfully controlled by adjusting the SL structures such as the N area density and SL period. Figure 5 shows the calculated conversion efficiency of IBSCs as a function of the CB–VB gap energy and the CB–IB gap energy. The calculation was based on the detailed balance model under the assumption of fully concentrated black-body (5760 K) irradiation. The closed symbols plotted in the figure indicate the energy gap relation of the fabricated SLs in which the bottom energies of the E_+ and E_- minibands estimated by PR are assumed to correspond to those of the CB and IB, respectively. From the figure, it is expected that IBSCs with a conversion efficiency of nearly 60% are achievable using the fabricated GaAs:N δ-doped SLs.

4. Conclusions

We have fabricated GaAs:N δ-doped SLs and demonstrated the control of energy configuration in the SLs by adjusting the structural parameters. Optical transitions due to the SL minibands related to the E_+ and E_- bands are clearly observed in the fabricated SLs. These miniband energies systematically depended on the N area density and period length of the SL, in other words, they were well-controlled. Conversion efficiency calculations based on the detailed balance model indicated that IBSCs with an efficiency of nearly 60% are achievable using the fabricated GaAs:N δ-doped SLs. In addition, annealing characteristics suggested that the abrupt distribution of N in δ-doped layers contributes to the enhancement of the E_+-related transitions in the SLs.

1) A. Luque and A. Marti, Phys. Rev. Lett. **78**, 5014 (1997).
2) A. Luque and A. Marti, Prog. Photovoltaics **9**, 73 (2001).
3) M. A. Green, Prog. Photovoltaics **9**, 123 (2001).
4) P. Palacios, J. J. Fernández, K. Sánchez, J. C. Conesa, and P. Wahnón, Phys. Rev. B **73**, 085206 (2006).
5) C. Tablero, Phys. Rev. B **74**, 195203 (2006).
6) A. Martí, E. Antolín, C. R. Stanley, C. D. Farmer, N. López, P. Díaz, E. Cánovas, P. G. Linares, and A. Luque, Phys. Rev. Lett. **97**, 247701 (2006).
7) R. Strandberg and T. W. Reenaas, J. Appl. Phys. **105**, 124512 (2009).
8) Y. Okada, T. Morioka, K. Yoshida, R. Oshima, Y. Shoji, T. Inoue, and T. Kita, J. Appl. Phys. **109**, 024301 (2011).
9) R. Oshima, Y. Okada, A. Takata, S. Yagi, K. Akahane, R. Tamaki, and K. Miyano, Phys. Status Solidi C **8**, 619 (2011).
10) P. G. Linares, A. Marti, E. Antolin, and A. Luque, J. Appl. Phys. **109**, 014313 (2011).
11) A. Luque, A. Martí, and C. Stanley, Nat. Photonics **6**, 146 (2012).
12) F. Wu, H. Lan, Z. Zhang, and P. Cui, J. Chem. Phys. **137**, 104702 (2012).
13) W. Shan, W. Walukiewicz, J. W. Ager, III, E. E. Haller, J. F. Geisz, D. J. Friedman, J. M. Olson, and S. R. Kurtz, J. Appl. Phys. **86**, 2349 (1999).
14) W. Walukiewicz, W. Shan, J. Wu, K. M. Yu, and J. W. Ager, III, in *Dilute Nitride Semiconductors*, ed. M. Henini (Elsevier, Amsterdam, 2005) Chap. 10, p. 325.
15) E. Cánovas, A. Marti, A. Luque, and W. Walukiewicz, Appl. Phys. Lett. **93**, 174109 (2008).
16) N. López, L. A. Reichertz, K. M. Yu, K. Campman, and W. Walukiewicz, Phys. Rev. Lett. **106**, 028701 (2011).
17) N. Ahsan, N. Miyashita, M. M. Islam, K. M. Yu, W. Walukiewicz, and Y. Okada, Appl. Phys. Lett. **100**, 172111 (2012).
18) N. Ahsan, N. Miyashita, M. M. Islam, K. M. Yu, W. Walukiewicz, and Y. Okada, IEEE J. Photovoltaics **3**, 730 (2013).
19) W. Shan, W. Walukiewicz, J. W. Ager, III, E. E. Haller, J. F. Geisz, D. J. Friedman, J. M. Olson, and S. R. Kurtz, Phys. Rev. Lett. **82**, 1221 (1999).
20) W. Shan, W. Walukiewicz, K. M. Yu, J. W. Ager, III, E. E. Haller, J. F. Geisz, D. J. Friedman, J. M. Olson, S. R. Kurtz, and C. Nauka, Phys. Rev. B **62**, 4211 (2000).
21) M. Geddo, T. Ciabattoni, G. Guizzetti, M. Patrini, A. Polimeni, R. Trotta, M. Capizzi, G. Bais, M. Piccin, S. Rubini, F. Martelli, and A. Franciosi, Appl. Phys. Lett. **90**, 091907 (2007).
22) A. Grau, T. Passow, and M. Hetterich, Appl. Phys. Lett. **89**, 202105 (2006).
23) J. D. Perkins, A. Mascarenhas, Y. Zhang, J. F. Geisz, D. J. Friedman, J. M. Olson, and S. R. Kurtz, Phys. Rev. Lett. **82**, 3312 (1999).
24) S. Noguchi, S. Yagi, D. Sato, Y. Hijikata, K. Onabe, S. Kuboya, and H. Yaguchi, IEEE J. Photovoltaics **3**, 1287 (2013).
25) S. Yagi, S. Noguchi, Y. Hijikata, S. Kuboya, K. Onabe, and H. Yaguchi, Jpn. J. Appl. Phys. **52**, 102302 (2013).
26) S. Yagi, S. Noguchi, Y. Hijikata, S. Kuboya, K. Onabe, Y. Okada, and H. Yaguchi, Appl. Phys. Express **7**, 102301 (2014).
27) D. E. Aspnes, Surf. Sci. **37**, 418 (1973).
28) J.-Y. Yeh, L. J. Mawst, and N. Tansu, J. Cryst. Growth **272**, 719 (2004).
29) E. V. K. Rao, A. Ougazzaden, Y. Le Bellego, and M. Juhel, Appl. Phys. Lett. **72**, 1409 (1998).
30) S. Francoeur, G. Sivaraman, Y. Qiu, S. Nikishin, and H. Temkin, Appl. Phys. Lett. **72**, 1857 (1998).
31) L. H. Li, Z. Pan, W. Zhang, Y. W. Lin, Z. Q. Zhou, and R. H. Wu, J. Appl. Phys. **87**, 245 (2000).
32) J. S. Harris, Semicond. Sci. Technol. **17**, 880 (2002).